RESEARCH ARTICLE OPEN ACCESS

Punching Shear High Strength Steel Fiber Reinforced Concrete Slabs

Vasant. B. Jatale[1] and L. G. Kalurkar[2]
[1]*(PG Student, Department of Civil Engineering, MGM's Jawaharlal Nehru Engineering College, Aurangabad/ Dr. B.A. Marathwada University, Aurangabad-431003, MS, India)*
[2]*(Assistant Professor, Department of Civil Engineering, MGM's Jawaharlal Nehru Engineering College, Aurangabad/ Dr. B.A. Marathwada University, Aurangabad-431003, MS,* India)

ABSTRACT
The punching shear behavior of High Strength steel fiber reinforced concrete slabs was investigated in the present study. Each of 24 square slabs was simply supported along four edges and loaded to failure under a concentrated load over a square area at the center. The test parameters were the effective span to depth ratio, volume fraction of 3 types of steel fibers p_f, slab thickness h, concrete strength f_{ck}, and size of load-bearing plate r. Test results indicate that the load-deflection curve of slabs exhibits four distinct regions that may be characterized by first cracking, steel yielding, and ultimate load. Within the scope of the test program, an increase in the values of p_f, h, or r was found to lead to an increase in both the punching shear strength and the ductility of the slab. The ultimate punching shear strength of the slabs was compared with the predictions of equations available in the literature and code equations for reinforced concrete. The British Standard CP110's equation was found to estimate the punching shear strength of the test specimens reasonably well.

I. INTRODUCTION

High Strength Fibres Reinforced concrete (HSFRC) is being increasingly used in civil engineering construction due to its improved resistance to cracking, fatigue, abrasion, and impact and its greater durability, than conventional reinforced concrete (Vondran 1991). Some examples are its applications in shotcrete, precast concrete products, pavements, concrete floors, seismic structures, and structural repair.

HSFRC-slab applications are suited for bridge deck slabs, industrial floors or in flat-slab construction where, besides resistance to fatigue or damaging dynamic forces, additional reinforcement is required to avoid punching shear failure due to concentrated loads. Although much research has been carried out on HSFRC ("State" 1982), little attention has been focused on the punching shear behavior of HSFRC slabs. As a result, the full economical benefits of steel fibers in such applications may not be realized.

In this study, an investigation has been carried out on the punching shear behavior of HSFRC slabs. Each of 24 square slabs was prepared and tested under a concentrated load. The load-deflection characteristics and cracking pattern of the slabs were observed and compared. The ultimate punching shear strength of the slabs was compared to predictions made using the equations available in the literature as well as those given in building codes ("Building" 1989; "Code" 1972; "Model" 1978; "Structural" 1985; "Standard" 1986) for the punching shear strength of reinforced concrete slabs.

II. TEST PROGRAM

Twenty four HSFRC slabs were tested as per IS-516. The parameters investigated included the effective span to depth ratio, aid volume fraction of three types of steel fiber at the volume fraction of 0.5% to 4%. The Volume fraction of different types fibres were taken at an interval of *0.5*%. The specimen placed on the steel stand by simply supported on Universal testing machine. One steel plate kept on the centre of slab whose dimension of 100x100x20 mm. The loads are increased gradually on the plate up to failure. The load deflection curves plotted directly on computer which is directly attach with universal testing machine. The graphs are plotted upto failure of specimen. The test results are described in table No. 1.

TABLE 1. Details of Test Specimens

Series (1)	Slab number (2)	*a/d* (3)	P_f (%) (4)	*h* (mm) (5)	f_{cu} (MPa) (6)	*r* (mm) (7)
1	HSFRC 1-1	27.2	0.31	35	50	100
1	HSFRC 1-2	40.9	0.31	35	50	100
1	HSFRC 1-3	54.5	0.31	35	50	100
2	HSFRC 2-1	40.9	0.50	35	50	100
2	HSFRC 2-2	40,9	1.00	35	50	100
2	HSFRC 2-3	40.9	1.50	35	50	100
2	HSFRC 2-4	40.9	2.00	35	50	100
3	HSFRC 3-1	65.2	0.31	22	50	100
3	HSFRC 3-2	25.1	0.31	57	50	100
3	HSFRC 3-3	20.5	0.31	70	50	100
4	HSFRC 4-1	40.9	0.31	35	35	100
4	HSFRC 4-2	40.9	0.31	35	65	100
5	HSFRC 5-1	40.9	0.31	35	50	200
5	HSFRC 5-2	40.9	0.31	35	50	150

Note: *dlh* = 0.625; p_s = 0.87 for all slabs.
f_{cu}= design cube compressive strength.

TABLE 2. Mix Design

Material	Proportion by weight	Weight in Kg/m^3
Cementatious Material	1	556
Fine Aggregate	1.26	701
Course Aggregate (12.5 mm)	1.87	1040
Water	0.27	150

The Thickness of slab *h*, concrete strength f_{ck} *and* width of the loading platen *r*. The slabs were accordingly grouped into five series as shown in Table 1.

For all the slabs, welded skeletal steel fabric with an average yield strength (corresponding to a total strain of 0.0035) of 70MPa and a grid size of 150 mm and bar diameters of 8 mm was used as the main reinforcement. The total volume fraction of main reinforcement was 0.3 for each slab, and the reinforcement was placed with the aid of plastic spacers such that the ratio of the effective depth to overall slab thickness *dlh* was 0,623 in each case.

Hooked-end steel fibers, Flat steel fibres and crimped steel fibre were used at different aspect ratio as fiber reinforcement. The specific yield strength of these fibers was 1,275 MPa each. The volume fraction of three types steel fibers was kept constant at 0.5%.

Ordinary Portland cement, Fly ash, Silica fume, natural sand, and crushed granite of 12.5 mm

TABLE 3. Test Results

Series (1)	Slab number (2)	f^1_c (MPa) (3)	P_{cr} (kN) (4)	P_y (kN) (5)	P_u (kN) (6)	δ_y (mm) (7)	δ_y (mm) (8)	δ_u/δ_y (9)
1	HSFRC 1-1	46.2	6.7	19.4	21.4	14.1	23.2	1.65
1	HSFRC 1-2	45.8	5.5	20.0	22.6	19.4	30.7	1.58
1	HSFRC 1-3	47.2	5.3	14.1	18.9	32.4	53.3	1.65
2	HSFRC 2-1	40.3	6.6	18.7	20.9	19.5	29.3	1.50
2	HSFRC 2-2	40.7	5.1	21.3	23.7	23.0	31.4	1.37
2	HSFRC 2-3	39.7	4.5	20.0	24.6	21.0	35.0	1.67
2	HSFRC 2-4	47.8	9.1	23.3	27.4	21.3	35.0	1.64
3	HSFRC 3-1	46.9	3.1	7.3	9.4	17.6	32.7	1.86
3	HSFRC 3-2	46.1	15.5	36.7	54.9	6.8	21.3	3.13

3	HSFRC 3-3	48.4	23.9	43.3	70.5	3.0	20.0	6.67
4	HSFRC 4-1	37.6	5.5	14.3	19.0	18.2	32.5	1.79
4	HSFRC 4-2	60.6	7.0	15.3	20.0	17.8	36.0	2.02
5	HSFRC 5-1	41.4	6.2	22.2	26.1	23.1	37.5	1.62
5	HSFRC 5-2	39.8	5.3	15.6	18.7	20.0	32.5	1.63
Note: f_c is assumed equal to $0.8f_{cu}$.								

Maximum size was used in the proportions shown in Table 2 to achieve the desired concrete strength. Admixtures were added in prescribed dosages in order to accelerate strength development and, in the case of slab HSFRC, to improve workability. The concrete compressive strength was determined using 100x100x100mm cubes, and the cylindrical compressive strength f_{cu} assumed as 0.8 times the cube compressive strength *fcu* at the time of testing of the slabs, is shown in Table 3.

Each slab was simply supported along four edges, with the corners free to lift as shown in Fig. 1. Load was applied centrally on the slab through a spherically seated plate by means of an MTS hydraulic jack. Which is used for obtain the actual deflection of the center of slab, five linear variable displacement transducers (LVDT) were attached, one at the midpoint of each line support and at the fifth transducer at the bottom of the slab at its center. The strains in the longitudinal reinforcement in two orthogonal directions were monitored by strain gages mounted at locations just outside the loading platten (see Fig. 1) prior to casting of slabs. The slab was loaded until the load punched through.

III. TEST RESULTS

General Behavior of Slabs

Fig. 2 shows the load versus deflection curves for all the slabs tested. The variations of steel stress with the applied load are shown in Fig. 3 for typical slabs. For each slab, the load-deflection curve is characterized by four distinct regions [see Fig. 2(*f*)]. Region I corresponds to the initial elastic un-cracked stage during which the applied load increased linearly with deflection. During this stage, the steel strains due to the applied load were small (see Fig. 3).

Upon the occurrence of cracks (region II), which first appeared at the bottom of the slab directly below the concentrated load, the slab stiffness is drastically reduced. The stress in the concrete was rapidly transferred to the steel reinforcement as the applied load increased gradually. In some

Test Setup and Instrumentation

Slabs, a short plateau was observed as the formation of cracks stabilized before the load picked up again. As the load further increased, more cracks appeared on the bottom of the slabs and were observed to propagate in a zigzag manner toward the edges of the slabs. Correspondingly, the steel strains increased rapidly, and eventually the yield strains were reached.

Further reduction in stiffness was observed as the applied load was increased (region III), and the yielding of steel reinforcement was deemed to have spread outwards to the edges of the slab. During this stage, the slab was observed to deflect excessively, and the increase in load was mainly due to membrane action of the slab. Near the ultimate load, the stiffness of the slab decreased rapidly and cracks started to appear on both the top and bottom surfaces of the slab in a circumferential direction around the loading plate. The loading plate began to punch through and finally, when the circumferential cracks became excessively wide, the load-carrying capacity of the slab dropped sharply.

The post peak region (region IV) indicated a further reduction in the load-carrying capacity of slabs. This reduction occurred in several steps, with spalling of the concrete from the bottom of the slab. Fig. 4 shows the crack patterns for some typical slabs after the tests.

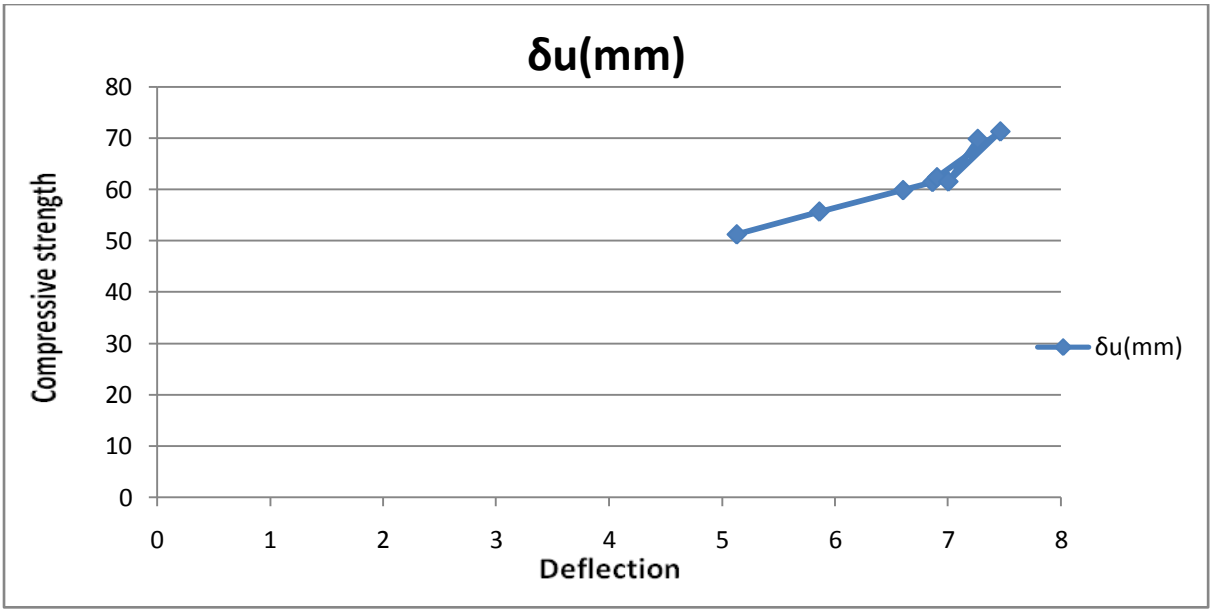

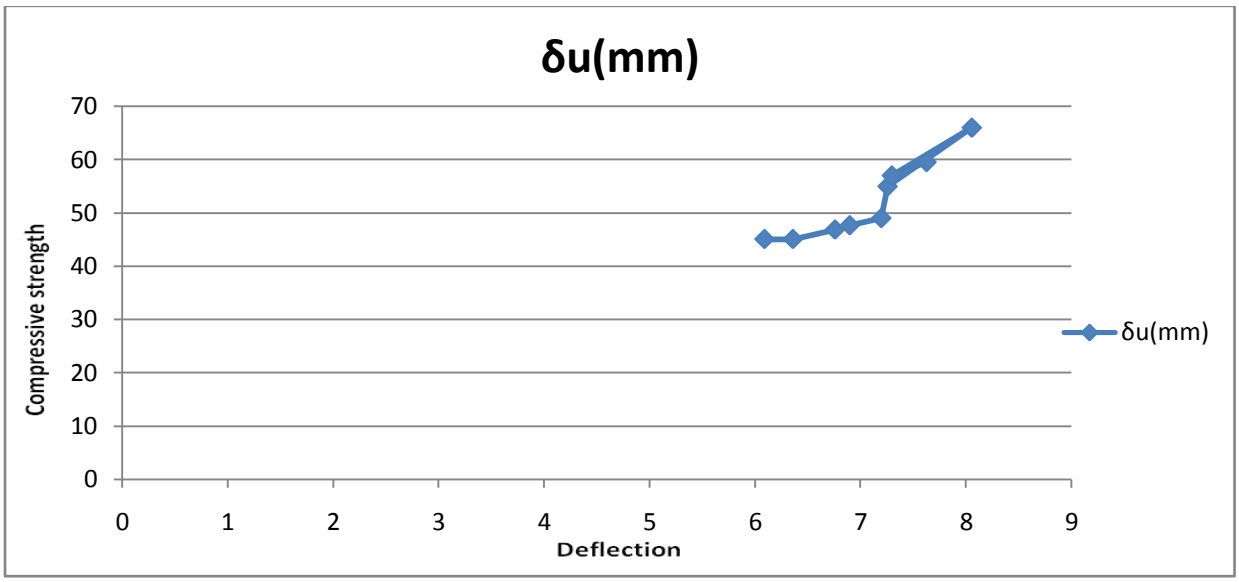

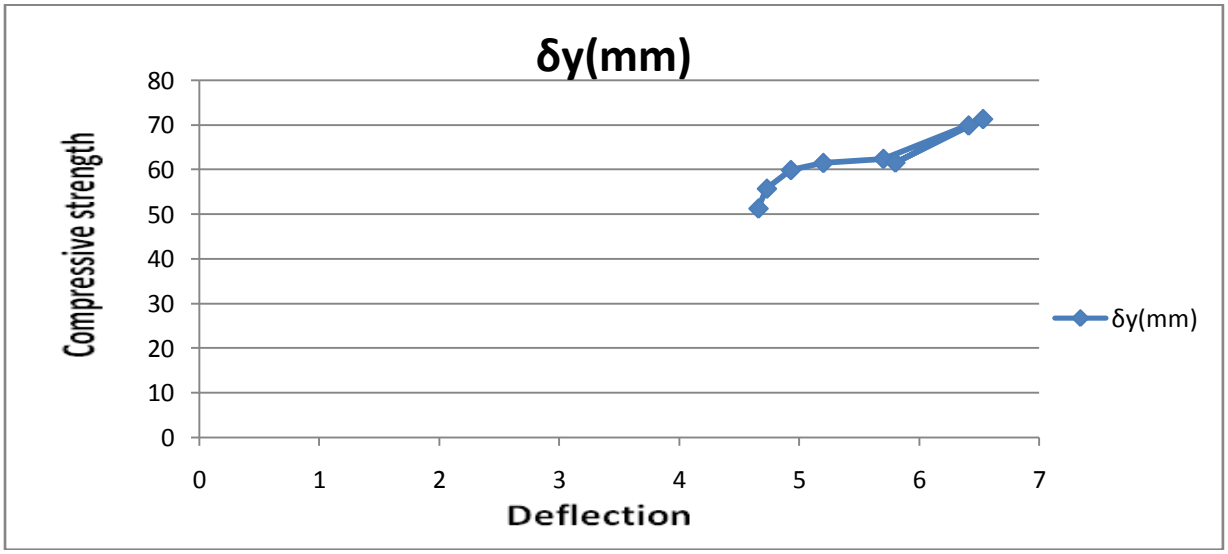

FIG.1. Load-Deflection Characteristics of HSFRC Slabs under Punching Shear Load

For all slabs, the critical punching-shear perimeter was found to occur at some distance away from the loading plate. Measurements on both the top and bottom surfaces of the slabs indicated that the critical perimeter formed, on average, at a distance of about 4.5 times the effective depth from the

FIG 2.Typical Crack Pattern of **HSFRC** Slabs after Punching Shear Failure:
(a) Slab **HSFRC** -1; (b) Slab **HSFRC** 2;(c) Slab **HSFRC** 3

Effects of Varying Test Parameters

Table 2 shows the observed cracking load P_{cr}, yield load P_y with corresponding deflection δ_y and ultimate load P_u with corresponding deflection 8_u for all slabs tested. The cracking load was determined from the load-deflection curve and confirmed by steel-strain readings; the yield load was obtained from the intersection of the linear portions of regions II and III [see Fig. 2(*f*)] of the load-deflection curve. Even though the value of P_y indicates a load level at which yielding of steel reinforcement in the slab has become sufficiently widespread, it does not necessarily agree with the load at which yielding of steel occurs just outside the loaded area (see Fig. 3). Table 3 also gives the values of δ_u / δ_y, which represent the ability of the slabs to sustain further deflection after first yield of steel reinforcement without any reduction in load-carrying capacity. These values can therefore be considered a measure of the ductility of the slabs.

The value of a/d does not affect the cracking load, yield load, or ultimate load significantly. This is because the curvature of the slab is proportional to the applied load and independent of the effective span of the slab. The smaller values of P_{cr}, P_y, and P_u for slab HSFRC 1-3 are probably due to a smaller loading area compared to slab dimension (i.e., smaller *rla*). The ductility of the slab is not influenced by the value of *a/d*as reflected by the values of δ_u/δ_y, which are about 1.6 for all slabs.

Series 2 slabs together with slab HSFRC C1-2, show that increasing the volume fraction of fibers generally leads to an increase in the values of P_{cr}, P_y, and P_u as well as δ_u/δ_y. The discrepancies observed in slabs HSFRC 1-2 and HSFRC 2-3 are due to higher and lower concrete compressive strengths, respectively.

Similarly, results for Series 3 slabs and slab HSFRC 1-2 indicate that increasing slab thickness leads to a higher cracking load, yield load, and

ultimate load. The ductility of the slabs, as defined by the value of δ_u/δ_y, increases with increasing slab thickness, although the observed values of δ_u, decrease with increasing slab thickness. These slabs had different aid ratios, but, as pointed out earlier, the value of *a/d* does not affect the results significantly, if at all, and the preceding deductions remain valid.

Series 4 slabs, when compared to slab HSFRC 1-2, indicate that the cracking load, yield load, ultimate load, and ductility are increased by increasing the compressive strength of fibrous concrete, although the results are not conclusive.

Increasing the loaded area (i.e., increasing r) resulted in higher values of P_{cn} P_y, and P_u, but did not affect the ductility of the slabs, as shown by the results of slabs HSFRC 5-1, HSFRC 5-2, and HSFRC 1-2.

IV. COMPARISON WITH AVAILABLE FORMULA AND CODE EQUATIONS

Although several studies (Ito et al. 1981; Narayanan and Darwish 1987; Swamy and AH 1982; Walraven et al. 1987) were carried out on the punching shear behavior of HSFRC slabs, only Narayanan and Darwish provided an equation for the prediction of the ultimate strength of HSFRC slabs in punching shear.

$$vu = \frac{P_u}{\xi_s u_b d} = 0.24 f_{sp} + 16_{\rho} + 0.41_{T_u} \rho_f d_f \frac{L}{D} \quad (1a)$$

where, respectively, u_b and ξ_s = the critical perimeter and the size effect factor, given as

$$u_b = \left(1 - 0.55 \rho_f d_f \frac{L}{C}\right)(4r + 3\pi h) \quad (1b)$$

and

$$\xi_s = 1.6 - 0.002h \quad (1c)$$

in which d_f=0.5, 0.75, and 1.0 for round fibers, crimped fibers, and duoform fibers, respectively;f_{sp} = splitting tensile strength of concrete [$f_{cu}/20 + 0.7 + (\rho_f \ d_f \ L/D)^{1/2}$(MPa)]; ρ = tensile steel ratio; ρ_f = volume fraction of steel fibers; $^{T}{}_{u}$= average fiber matrix interfacial bond stress; *L*= length of fibers; and *D*=diameter of fibers. Narayanan and Darwish recommend that $^{T}{}_{u}$be taken as 4.15 MPa in using (1*a*). In (1*c*), ξ_s is taken as not less than 1 and *h*is in millimeters. In applying (1) for the test specimens in the present study, d_f was taken as equal to 1.0, since hook-ended steel fibers were used.

On the other hand, code equations do not in general account for the contribution of steel fibers toward the ultimate punching shear strength directly. Instead, the contribution of fibers can be viewed by its effect on the tensile strength of concrete, which could be related to the compressive strengthf'_c or f_{cu}. In using the code equations, all the factors of safety and strength capacity reduction factors were assumed to be equal to unity. The following code equations were used in the present study.

The American Concrete Institute (ACI) equation ("Building" 1989), which is

$$v_u = \frac{P_u}{4(r+d)d} = 0.332 f'_c{}^{1/2} \text{ (Mpa)} \quad (2)$$

The British Standards Institution CP110 equation ("Code" 1972) is

$$v_u = \frac{P_u}{\xi_s(4r+3\pi h)d} = 0.27\,(100\, f_{cu})^{1/3} \text{ (Mpa)} \quad (3)$$

whereξ_s is as given in (1*c*).

The British Standards Institution BS8110 equation ("Structural" 1985) is

$$v_u = \frac{P_u}{4(r+3d)d} = 0.79\left(100\rho\frac{f_{cu}}{25}\right)^{1/3}\left(\frac{400}{d}\right)^{1/4} \text{(Mpa)} \quad (4)$$

whereρ,f_{cu}, and (400/*d*) are limited to 0.03, 40 MPa, and 1.0, respectively. In the present study, however, the value of $f_{cu}$is not limited, so the effect of steel fibers can be considered.

The CEB-FIP model code equation ("Model" 1978) is

$$v_u = \frac{P_u}{\xi_s(4r+\pi d)d} = 0.084\,(1+50\rho)\, f'_c{}^{2/3} \text{(Mpa)} \quad (5)$$

whereξ_s = 1.6 - 0.001*d*, with ξ_s taken as not less than 1.0 and *d*is in millimeters. In (5), ρ, which is calculated for a slab width of (*r* + 5*d*)is taken to be not more than 0.02.

The Japan Society of Civil Engineers (JSCE) equation ("Standard" 1986) is

$$v_u = \frac{P_u}{4(r+\pi d)d} = 0.188\beta_d\beta_p\beta_r{}^{1/2} \text{(Mpa)} \quad (6)$$

whereβ_d = (l,000/*d*)$^{1/4}\beta_p$, = $(100\rho)^{1/3}$; and β_r = 1 + 1/(1 + *r/d*), with the values of $\beta_d$and $\beta_p$each limited to 1.5.

Table 4 shows a comparison of the punching shear strength of the test specimens with the predictions of Narayanan and Darwish's equation (1987) and the code equations. The average and standard deviation of the ratio of test values to predicted values by the various equations is shown in graphical form in Fig. 5. Narayanan's equation generally overestimates the punching shear strength of the specimens tested. Of the code equations, the JSCE equation is the most conservative and the CP110 equation predicts behavior with the best accuracy and the least standard variation. The BS8110, and the AC1 and CEB-FIP equations predict, on average, 10% lower strength than the test values, with a standard deviation of above 20%.

V. CONCLUSIONS

Within the scope of the study, the following conclusions may be drawn. The load-deflection curve of SFRC slabs under a concentrated load exhibits four distinct regions:

(1) The initial elastic uncracked region;
(2) The crack development region;
(3) The post yielding region; and
(4) The post-peak region.

The critical perimeter for punching shear failure in SFHSRC slabs forms at a distance of about 4.5 times the effective depth from the perimeter of the loading platen, with the shear plane inclined at 20^0-60^0 to the plane of the slab.

Punching shear failure in HSFRC slabs is preceded by yielding of steel reinforcement and is accompanied by cracks mainly in the radial direction and partly in the circumferential direction.

An increase in the volume fraction of steel fibers, slab thickness, compressive strength of fiber concrete, or the loaded area generally leads to an increase in the cracking load, yield load, ultimate load, and ductility of HSFRC slabs.

The punching shear strength of HSFRC slabs in the present study were predicted with reasonable accuracy using the BS-CP110 equation for reinforced concrete,

VI. ACKNOWLEDGMENT

The work upon which the present paper is based was supported by the National University of Singapore Research Grant RP880646,

APPENDIX I.
REFERENCES

[1] "Building code requirements for reinforced concrete and commentary."(1989). ACI 318-89/ACI318R-89.American Concrete Institute, ACI, Detroit, Mich.

[2] "Code of practice for the structural use of concrete."(1972). CP110, Part 1, British Standards Institution, London, England.

[3] Ito, K., Hirasawa, I., and Aichi, I. (1981)."Punching shear strength of steel fiber reinforced concrete slab."Trans., Japan Concrete Inst., Tokyo, Japan, 3, 267-272.

[4] "Model code for concrete structures."(1978). International System of Unified Standard Codes of Practice for Structures, Vol. II, Bull, *d'*Information No. 124/125-E, 3rd Ed., Comite Euro-International du Beton—Federation Internationale de la Precontrainte (CEB-FIP), London, England/Paris, France.

[5] Narayanan, R., and Darwish, I. Y. S. (1987). "Punching shear tests on steel fibre reinforced micro concrete slabs." Magazine of Concr. Res., 39(138), 42-50.

[6] "Standard specifications for design and construction of concrete structures, part 1 (design)." (1986). Japan Society of Civil Engineers, Tokyo, Japan.

[7] "State-of-the-art report on fiber reinforced concrete." (1982). ACI544.IR-82, American Concrete Institute, ACI, Detroit, Mich.

[8] "Structural use of concrete; part 1, code of practice for design and construction."(1985).

[9] BS8110, British Standards Institution, London, England.

[10] Swamy, R. N., and Ali, S. A. R. (1982). "Punching shear behavior of reinforced slab-column connection made with steel fiber concrete." J, ACI, 79(5), 392-406.

[11] Vondran, G. L. (1991). "Applications of steel fiber reinforced concrete." Concr. Int.: Design & Constr., 13(11), 44-49.

[12] Walraven, J., Pat, T., and Markov, I. (1986). "The punching shear resistance of fibre reinforced concrete slabs." 3rd Int. Symp. Developments in fibre reinforced cement and concrete, Vol. 2, Paper 8.9, RILEM Technical Committee TFR49, England, U.K.

APPENDIX II.
NOTATIONS

The following symbols are used in this paper:

a = effective span of test specimen;
d = average effective depth to tension reinforcement;
f'_c = cylinder compressive strength of (fiber) concrete;
f_{cu} = cube compressive strength of (fiber) concrete;
h = slab thickness;
P_{cr} = cracking load ;
P_y = yield load;
P_u = ultimate load;
r = width of loading platen;
u_b = critical punching shear perimeter;
v_u = ultimate punching shear stress;
δ_y = deflection at yield load;
δ_u = deflection at ultimate load;
ξ_s = size effect factor;
ρ = tension reinforcement ratio;
p_f = volume fraction of steel fibers; and
p_s = volume fraction of tension reinforcement.